Elastic properties of polycrystalline Al and Ag films down to 6 mK

A. D. Fefferman, R. O. Pohl, and J. M. Parpia*
Department of Physics, Cornell University, Ithaca, New York 14853, USA

(Received 28 February 2010; revised manuscript received 17 June 2010; published 20 August 2010)

The elastic properties of as-deposited high-purity micron-thick polycrystalline Al and Ag films were measured with the double paddle resonator technique down to 6 mK, and important differences from previous measurements were found. The lowest internal frictions (Q^{-1}) observed were 3×10^{-5} in Al and 4×10^{-5} in Ag, indicating that these films can contribute substantially to the damping of mechanical resonators, even at very low temperatures. In Al, we also observed agreement between the relative change in sound speed $\delta v/v_0$ and Q^{-1} and the predictions of the tunneling model for an amorphous superconductor well below T_c. Dislocation kinks tunneling between local minima in a kink-Peierls potential modulated by disorder could form the broad distribution of tunneling states required by the tunneling model. However, previous measurements have shown that the thermal conductivity, heat capacity, and heat release of polycrystalline bulk metal and films are not in agreement with the tunneling model predictions.

DOI: 10.1103/PhysRevB.82.064302 PACS number(s): 62.40.+i, 63.20.kp, 63.50.−x, 68.60.Bs

I. INTRODUCTION

Many mechanical resonators, from nanoscale beams to gravitational wave detectors, are composed of or are coated with polycrystalline or amorphous material, and it is important to understand the contribution of the disordered material to the damping.[1–7] It was shown in Ref. 8 that many polycrystalline metal films have an internal friction in the glassy range $2\times10^{-4}<Q^{-1}<2\times10^{-3}$ between 0.1 K and a few kelvins, as is observed in almost all amorphous solids.[9,10] In this paper, we present elastic measurements on micron-thick polycrystalline Al and Ag films at 5.5 kHz from 100 K to below 10 mK. Near 10 mK, $Q^{-1}\approx3\times10^{-5}$ in Al and $Q^{-1}\approx4\times10^{-5}$ in Ag, both of which are still an order of magnitude greater than Q^{-1} in annealed bulk Al below 100 mK.[8] Thus defects play an important role in these polycrystals, even at very low temperatures.

The results of previous elastic measurements on polycrystalline Al and Ag contrast with the present results in both magnitude and temperature dependence. Surprisingly, the variation in Q^{-1} of the samples measured by different researchers is not clearly correlated with dislocation density. Also in contrast with the findings of others, we observed good agreement between the elastic properties of our Al film and the prediction of the tunneling model (TM) for an amorphous superconductor well into the superconducting state. The two-level systems (TLSs) presumed by the tunneling model could be formed by tunneling dislocation kinks in the polycrystal.[11] However, it is not clear how to reconcile the predictions of this model with previous thermal measurements on polycrystals, even if a nonuniform distribution of two-level system asymmetries is assumed.

II. THEORY

In perfect dielectric crystals at very low temperatures, the relative change in sound speed $(v-v_0)/v_0\equiv\delta v/v_0=-d'T^4$, where d' is a constant and v_0 is the sound speed at an arbitrary reference temperature T_0.[12] The internal friction Q^{-1} is expected to decrease quickly until it is limited by nonintrinsic effects such as clamping loss. Disorder within a crystal alters the temperature dependence of $\delta v/v_0$ and Q^{-1}. In fully disordered, amorphous solids, the TM (Refs. 13 and 14) has been rather successful in describing the low-temperature properties of glass.

A. Two-level systems

We briefly summarize the relevant predictions of the TM so that they can be compared with the results of our measurements on the metal films. The TM presumes the existence of low-energy excitations that interact with phonons in the glass, as well as with electrons in the case of metallic glasses.[15,16] The low-energy excitations are thought to be formed by atoms or groups of atoms tunneling between nearly degenerate states and are approximated by TLSs. It is assumed that the ensemble of tunneling TLS has a broad distribution of parameters with spectral density

$$P(\Delta,\Delta_0)=\frac{P_0}{\Delta_0}, \tag{1}$$

where P_0 is a constant and the TLS asymmetry Δ is defined in Fig. 1. The TLS tunneling amplitude is given by

$$\Delta_0\approx\hbar\Omega\exp(-\lambda), \tag{2}$$

where

$$\lambda=d(2mV_0/\hbar^2)^{1/2}, \tag{3}$$

$\hbar\Omega$ is approximately the mean ground-state energy for the potential wells in the TLS if they were isolated, d is the separation in configuration space between the minima of the two wells, m is the mass of the tunneling entity, and V_0 is the height of the TLS barrier. The TLS energy splitting is given by $E=\sqrt{\Delta^2+\Delta_0^2}$. A heat capacity

$$C_{\mathrm{TLS}}=\frac{E^2}{4k_BT^2}\mathrm{sech}^2\left(\frac{E}{2k_BT}\right) \tag{4}$$

associated with each TLS is obtained by differentiating the mean energy of a TLS with respect to temperature. Integrat-

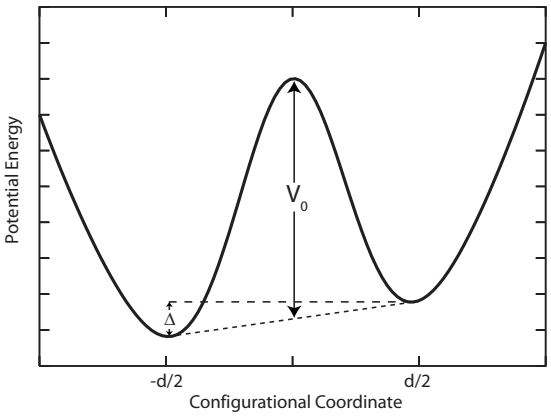

FIG. 1. A generic TLS is characterized by an asymmetry, Δ, a well separation d, a barrier height V_0, and a tunneling amplitude Δ_0. The exact dependence of Δ_0 on d and V_0 depends on the precise shape of the potential, which is generally unknown.

ing Eq. (4) over the distribution of tunneling states leads to a linear temperature dependence of the heat capacity.

B. Tunneling model: Elastic properties

Here we give an overview of the physics followed by a summary of quantitative predictions. TLS-phonon and TLS-electron interactions contribute to the acoustic observables through relaxational or resonant processes. In the resonant process, phonons at ω_0 introduced by an external source are scattered by TLS with energy splitting $E=\hbar\omega_0$, driving the phonon population toward the thermal equilibrium distribution. The resonant contribution to Q^{-1} due to TLS with particular Δ and Δ_0 is proportional to the phonon-scattering rate, and the resonant contribution to $\delta v/v_0$ can be obtained from Q^{-1} using the Kramers-Krönig relation.[17,18] Although the resonant contribution to Q^{-1} is small for the temperature and frequency range of our measurements, the resonant contribution to $\delta v/v_0$ is substantial because the Kramers-Krönig relation involves integration over all frequencies.

In the relaxational process, drive phonons interact with TLS with all energy splittings by perturbing the TLS asymmetry Δ and thus changing the energy splitting. The ensemble of TLS is then no longer in thermal equilibrium, and thermal phonons, or electrons in the case of a normal metal, interact with the TLS, driving them back toward thermal equilibrium. Since re-equilibration of the TLS involves motion of particles in the lattice, it contributes to the stress in the lattice for a given strain, thus contributing to the modulus. The real part of the change in the modulus is proportional to $\delta v/v_0$ and the imaginary part of the change in the modulus is proportional to Q^{-1}.

The predictions of the TM are derived in mathematical detail in Refs. 17 and 19. Here we summarize the relevant results. The TLS relaxation rate due to quantum-mechanical tunneling stimulated by phonons is[20]

$$\tau_{ph}^{-1} = \left(\frac{\gamma_l^2}{v_l^5} + 2\frac{\gamma_t^2}{v_t^5}\right)\frac{E\Delta_0^2}{2\pi\rho\hbar^4}\coth(E/2k_BT), \tag{5}$$

where γ is the change in TLS asymmetry per unit strain, ρ is the density of the solid, v is the sound speed, and l and t stand for longitudinal and transverse phonon polarizations, respectively. Unpaired electrons contribute to the TLS relaxation rate a term[20]

$$\tau_{el}^{-1} = \frac{\pi}{4\hbar}K^2\left(\frac{\Delta_0}{E}\right)^2 E\coth(E/2k_BT), \tag{6}$$

where K is the dimensionless electron-TLS coupling constant. Below the transition temperature of a superconducting glass the electron-driven TLS relaxation rate is exponentially suppressed.[20] The total relaxation rate is defined as $\tau^{-1}=\tau_{ph}^{-1}+\tau_{el}^{-1}$. In Table I,[22] we give the asymptotic forms of Q^{-1} and $\delta v/v_0$ for the cases in which TLS relaxation is dominated by electrons or phonons. The constant $a=(\gamma_l^2/v_l^5+2\gamma_t^2/v_t^5)k_B^3/2\pi\rho\hbar^4$ is the prefactor of τ_{ph}^{-1}, ω is the driving frequency, and $C=P_0\gamma^2/\rho v^2$ is the tunneling strength.

TABLE I. Limiting cases of the acoustic response of an amorphous solid for $\hbar\omega \ll k_BT$. The total $\delta v/v_0$ and Q^{-1} are obtained by adding the resonant and relaxational contributions. T_{CO} is the crossover temperature at which $\omega\tau=1$ for the dominant tunneling states. It is standard to simplify some of the contributions to $\delta v/v_0$ by referring them to temperatures (T_0', T_0'', and T_0''') at which the contribution to $\delta v/v_0$ is taken to be zero. See Refs. 17 and 21 for the expressions for the absolute sound speed shift. See text for a definition of other parameters in the table. The total response is given in Figs. 6 and 7 for a particular choice of parameters and with $\tau=\tau_{ph}$. In this case, the relaxational contribution to $\delta v/v_0$ for $T \ll T_{CO}$ and the resonant contribution to Q^{-1} are negligible, yielding a $2:(-1)$ slope ratio of $\delta v/v_0$ below and above T_{CO} (Fig. 7).

Interaction	Quantity	$T \ll T_{CO}$	$T \gg T_{CO}$
Resonant	$\frac{\delta v}{v_0}$	$C\ln(\frac{T}{T_0'})$	
Relaxational, $\tau=\tau_{ph}$ (dielectric) or $\tau\approx\tau_{ph}$ (superconductor)	$\frac{\delta v}{v_0}$	$-\frac{(2\pi)^6}{315}Ca^2\frac{T^6}{\omega^2}$	$-\frac{3}{2}C\ln(\frac{T}{T_0''})$
Relaxational, $\tau\approx\tau_{el}$ (normal metal)	$\frac{\delta v}{v_0}$	$-\frac{\pi^4}{180}CK^4(\frac{k_BT}{\hbar\omega})^2$	$-\frac{1}{2}C\ln(\frac{T}{T_0''})$
Resonant	Q^{-1}	$\pi C\tanh\frac{\hbar\omega}{2k_BT}$	
Relaxational, $\tau=\tau_{ph}$ (dielectric) or $\tau\approx\tau_{ph}$ (superconductor)	Q^{-1}	$\frac{\pi^4}{12}Ca\frac{T^3}{\omega}$	$\frac{\pi}{2}C$
Relaxational, $\tau\approx\tau_{el}$ (normal metal)	Q^{-1}	$\frac{\pi^3}{24}CK^2\frac{k_BT}{\hbar\omega}$	$\frac{\pi}{2}C$

The TM has been successful in describing the low-temperature elastic properties of the prototypical dielectric glass, SiO_2, down to 10 mK.[23,24] This theory also does a fairly good job predicting the observed behavior of metallic and superconducting glasses,[20,25] although the agreement breaks down at high strains and low temperatures.[26] Also, the effects of the electron-TLS interaction do not seem to be fully captured by the electronic contribution to the TLS relaxation rate. In the simplest picture, the fast electron-driven relaxation causes the suppression of T_{CO} (Table I) to a very low value.[27] Reference 12 briefly reviews some more advanced treatments of electron-TLS interactions and gives several relevant references. The elastic properties of chemically disordered crystals also have many of the features predicted by the TM: for sufficiently high impurity concentrations a broad temperature-independent Q^{-1} plateau as well as a sharp decrease at the lowest temperatures is observed.[28]

C. TLS in polycrystals

Though polycrystals are not fully disordered, dislocation kinks in the crystallites may contribute to the elastic properties. In Ref. 11, Vegge *et al.* calculate the effective mass and barrier height for jogs and kinks in Cu screw dislocations. Jogs were shown to have a barrier for migration of 150 K and an effective mass of $0.36M_{Cu}$, leading to a suppression of the tunneling amplitude by a factor $e^{-\lambda}=10^{-14}$. Thus the tunneling of jogs is unlikely, and thermally activated motion is also unlikely at temperatures well below 150 K. However, the calculations for the dislocation kink in Cu yielded an activation energy for kink motion of 2 mK. Thus thermally activated motion in Cu is likely even at the lowest temperatures of our experiment. This very low barrier height was attributed to the width of the dislocation kinks. The spatial extension of the kink also led to a low effective mass $M_{Cu}/130$. The resulting WKB factor was $e^{-\lambda}=0.985$, indicating that the tunneling rate would be close to the attempt frequency Ω. Thus dislocation kinks are the most likely tunneling entity in pure fcc metals.

The effective mass and barrier for Al are expected to be larger than that for Cu because the bonding in Al is more covalent (making the rearrangement of bonds during kink migration more expensive) and the dislocation core is not split into partials as thoroughly—almost certainly overcompensating for the lighter Al mass. However, the qualitative result of this calculation for Cu, namely, that the barriers and effective masses for the dislocation kink are small enough so that tunneling or thermal activation is possible, should hold for Al as well.[29] Though the Ag lattice may be even more similar to Cu than Al in this regard, the presence of unpaired electrons in Ag would lead to faster relaxation of TLS than in superconducting Al.

The barrier for dislocation kinks is expected to be periodic in a perfect crystal. Static strains due to interactions with other defects are expected to introduce variations in the kink potential energy on a length scale much greater than the lattice spacing—naturally leading to a slowly modulated sinusoidal potential. The two lowest minima in this modulated sinusoid are thus rather similar in energy, and tunneling states formed from these pairs of minima lead to a prediction of an excess of nearly symmetric ($\Delta \ll \Delta_0$) TLS.[29]

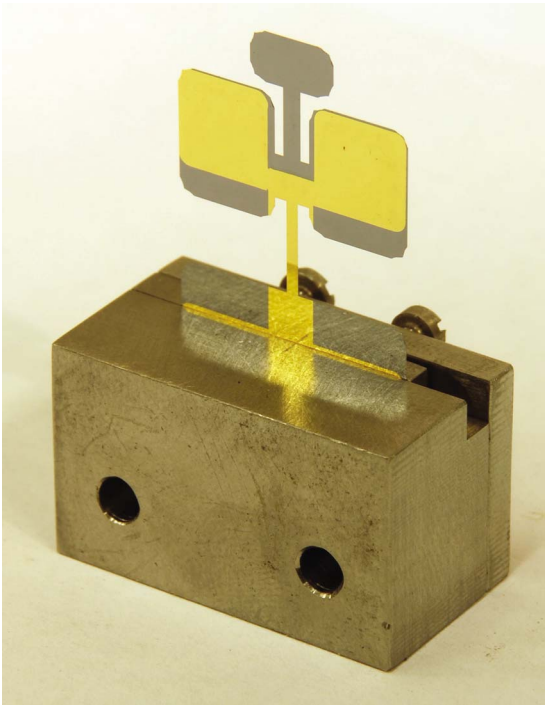

FIG. 2. (Color online) Photograph of a "bare" silicon double paddle resonator in the invar clamp assembly (Ref. 30). The sample to be studied must cover the neck, where the strain is concentrated (Fig. 3).

III. EXPERIMENT

A. Substrate and deposited films

Single-crystal silicon double paddle resonators formed the substrates for our metal film measurements. These resonators, described in detail in Ref. 1, are etched from wafers of 300-μm-thick Si with the geometry shown in Fig. 2. Unlike in Ref. 1, an epoxy-free clamp was used in the present work, as shown in Fig. 2. The clamp assembly is made of invar so that its thermal expansion is small and similar to that of Si. The Si resonator can be operated in a number of modes but the second antisymmetric torsional (AS2) mode near 5.5 kHz has by far the lowest dissipation,[1] making it ideal for measurements of the elastic properties of paddle coatings. The displacement profile and strain energy density for the AS2 mode calculated using the finite element method are shown in Fig. 3.[30]

As shown in Fig. 2, a gold film was deposited onto part of one side of the paddle for electrostatic drive and detection of the motion. The high strain regions near the upper torsion rod (the "neck") (Fig. 3) were avoided so that the gold film did not contribute to Q^{-1} of the resonator. We found $Q_{bare}^{-1} \approx 2\times 10^{-8}$ below 10 K for the paddle with only a gold film (to be discussed later).

Electron-beam deposition was used to deposit a thin layer of Cr for adhesion followed by a 1-μm-thick layer of pure Ag onto the bare paddle. A mask was used so that Cr and Ag

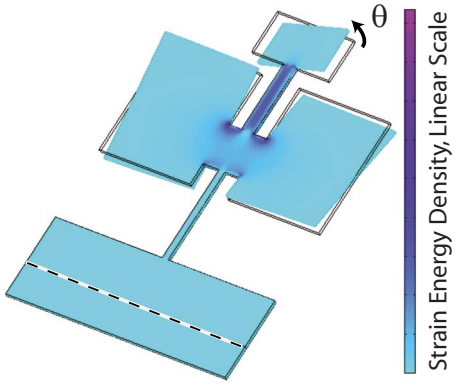

FIG. 3. (Color online) Displacement profile and strain energy density of the AS2 mode of the silicon double paddle resonator (Ref. 30). The double lines show the equilibrium position of the wings and head and the black and white dashed line indicates the edge of the clamp. The angle θ is used to specify the amplitude of motion.

were deposited only onto the neck of the paddle where the strain energy is concentrated.

After making measurements on the Ag film, the Ag was stripped with nitric acid and the Cr was stripped with 85% by weight phosphoric acid at 160 °C. Phosphoric acid is known to etch Si slowly or not at all, and nitric acid alone is also not an effective Si etchant.[31,32] Film stripping typically results in changes in Q^{-1} of the bare resonator of 3×10^{-9}, compared with $Q^{-1}>10^{-7}$ measured for our resonators with Al or Ag films (Fig. 5). It is thus very unlikely that this etching step significantly degraded the Q of the resonator.

Thermal deposition was used to coat the entire surface without gold film with a 5N purity Al film 985 nm thick, as measured by a quartz-crystal monitor. The tooling factor was checked using a profilometer, and the estimated error in the thickness measurement is less than 10%. The deposition rate was $\approx$50 nm/min and the pressure during deposition was less than 10^{-6} Torr. The deposition stage was coupled to a heat sink cooled by circulating liquid nitrogen, and this cooling scheme resulted in high-quality films in the past. During deposition, thermal radiation from the evaporator typically elevated the temperature of the deposition stage to $\approx$200 K. The resonator was kept in its invar clamp during the deposition to avoid clamping the resonator directly to the evaporator stage and risking scratches in the gold film electrodes. The thermal resistance between the double paddle resonator and the evaporator stage probably resulted in substantial elevation of the resonator temperature relative to the evaporation stage. The relatively high temperatures at which deposition took place resulted in some large scale defects in the Al film (e.g., peeling on a 100 μm length scale). Such large-scale defects might result in a higher background dissipation but a temperature-dependent contribution is not expected. In both the Al and Ag films, considerable strain must have been introduced by differential thermal contraction of the substrate and the film. While the relative change in the linear dimension of a silicon sample is $\Delta L/L\approx2\times10^{-4}$ between room temperature and low temperatures[33] for Al and Ag $\Delta L/L\approx4\times10^{-3}$.[34]

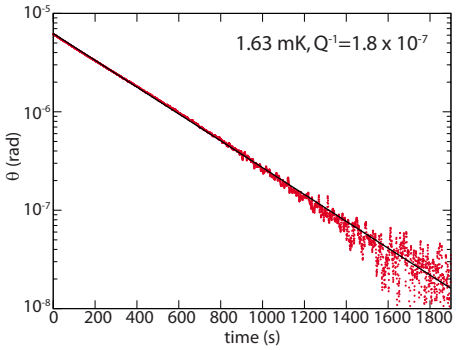

FIG. 4. (Color online) Example-free decay of composite Si/Ag film double paddle resonator at 1.63 mK and best-fit line. The angle θ is indicated in Fig. 3. The thicknesses of the Si and Ag are 300 μm and 1 μm, respectively.

B. Detection scheme

Due to the long mechanical time constants of the resonators, even when coated with a metallic film, it was not practical to use the frequency sweep technique that was applied in Ref. 23. Instead, the free decay of the resonator motion was measured using an SR830 digital lock-in amplifier, with the reference frequency stabilized by a Stanford FS700 LORAN frequency standard. We set the reference frequency f_{ref} slightly off the resonant frequency f so that $f-f_{ref}>\tau_{decay}^{-1}$, where τ_{decay} is the decay time of the resonator motion. We obtained Q^{-1} from the measurement of τ_{decay} and obtained $f-f_{ref}$ from the evolution of the phase of the motion relative to the reference signal. The resonant frequency f is then related to $\delta v/v_0$ of the film as shown below.

A sample decay of the amplitude of the resonator with the Ag film at 1.6 mK is shown in Fig. 4. The slope of the ring down on this log-linear scale is constant to a high precision over more than an order of magnitude in amplitude, indicating that we are operating in the linear regime and strain heating is negligible. At high amplitudes, the lock-in data agreed with data obtained with the ac voltmeter function of a PAR 124, further verifying our results.

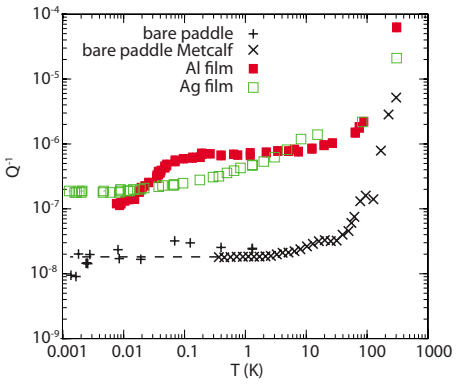

FIG. 5. (Color online) Dissipation of the bare Si substrate and composite resonators with Ag or Al films. The dashed line indicates Q_{bare}^{-1} used in Eq. (7). The points labeled "Metcalf" are from a private communication (Ref. 30). The variation in Q^{-1} between different Si resonators of similar design is small as can be verified by comparison of our results with those of Metcalf.

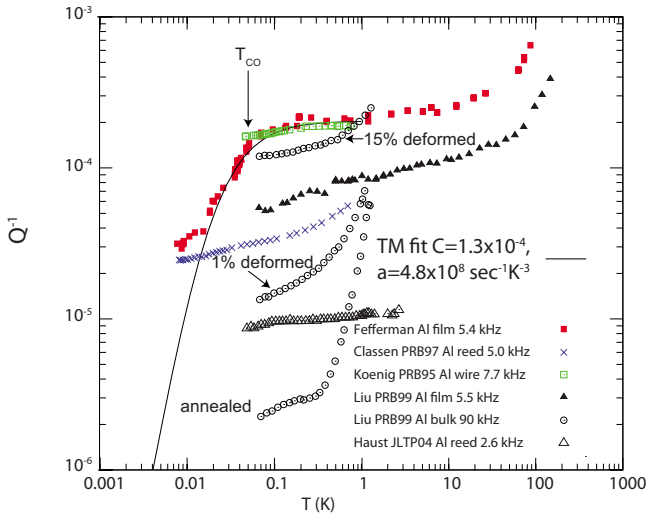

FIG. 6. (Color online) Measurements of Q^{-1} for several Al samples of different types: the film studied in the present work, the reed studied by Classen *et al.* (Ref. 12), the wire studied by Koenig *et al.* (Ref. 37), the film and bulk samples studied by Liu *et al.* (Ref. 8), and the reed studied by Haust *et al.* (Ref. 38). The TM prediction that best fits our measurements of Q^{-1} in Al is shown (solid line) and the crossover temperature T_{CO} is labeled (Table I).

C. Analysis method

The internal friction of a thin film is related to that of the composite paddle and the bare substrate according to the equation[35]

$$Q_{film}^{-1} = \frac{G_s t_s}{3 G_f t_f}(Q_{paddle}^{-1} - Q_{bare}^{-1}) \tag{7}$$

for $t_f \ll t_s$, where G_s (G_f) is the shear modulus of the substrate (film) and t_s (t_f) is the thickness of the substrate (film). Although the direction of the shear stress varies throughout the neck of double paddle resonator, the shear modulus of silicon varies with direction by only about 30%.[36] Thus we used the maximum silicon shear modulus, 80 GPa, without incurring much error. For the metal films, the bulk shear moduli were used: $G_{Ag}=30$ GPa and $G_{Al}=26$ GPa. The results are shown in Fig. 6 along with the results of other experiments and are discussed in Sec. IV A.

Equation (7) neglects contributions to Q_{paddle}^{-1} from poor bonding, contamination or disorder at the interface between the film and the substrate and from contamination on the outer surface of the film. Generally it is thought that these contributions are small and temperature independent. For example, in a similar study of metal films that did not extend to such low temperatures[8] it was shown that Q_{paddle}^{-1} was linear in the film thickness for Au films as thin as 10 nm deposited on 3 nm Cr sticking layers. If an interfacial term were significant for these gold films, one would expect the dependence of Q_{paddle}^{-1} on film thickness to weaken for small thicknesses. We take this result as evidence that interfacial disorder or contamination is not likely to be significant for our Al film. We expect the peeling in our film to yield a small temperature-independent contribution to Q_{paddle}^{-1}.

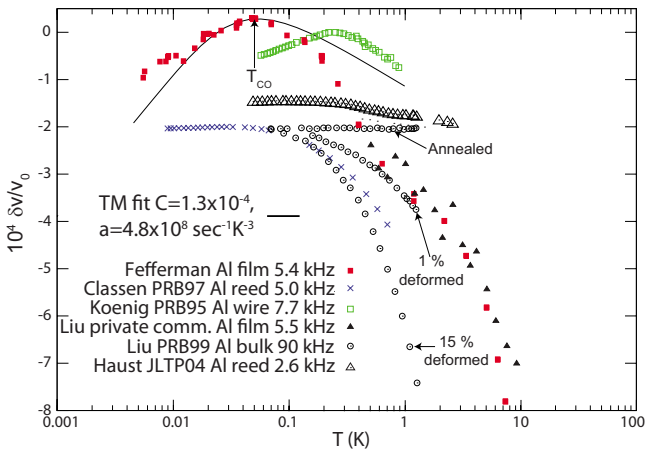

FIG. 7. (Color online) Measurements of $\delta v/v_0$ for several Al samples of different types: the film studied in the present work, the reed studied by Classen *et al.* (Ref. 12), the wire studied by Koenig *et al.* (Ref. 37), the film and bulk samples studied by Liu *et al.* (Ref. 8), and the reed studied by Haust *et al.* (Ref. 38). The TM prediction for the same parameters used in Fig. 6 is shown (solid line) and the crossover temperature T_{CO} is labeled (Table I).

The $\delta v/v_0$ for our Al film was determined by subtracting the contribution from the bare silicon substrate from the $\delta v/v_0$ of the composite paddle according to the formula[39]

$$\left(\frac{\delta v}{v_0}\right)_{film} = \frac{1}{3}\frac{G_s t_s}{G_f t_f}\Delta\left(\frac{\delta f}{f_0}\right) + \left(\frac{\delta v}{v_0}\right)_{bare}, \tag{8}$$

where

$$\Delta\left(\frac{\delta f}{f_0}\right) = \left(\frac{\delta f}{f_0}\right)_{paddle} - \left(\frac{\delta f}{f_0}\right)_{bare} \tag{9}$$

and $\delta v/v_0 = \delta f/f_0$ for negligible thermal expansion. The results are shown in Fig. 7 along with the results of other experiments and are discussed in Sec. IV A.

IV. RESULTS AND DISCUSSION

A. Present work: Aluminum

The results for the dissipation of the bare paddle and the paddle coated with the Ag and Al films are shown in Fig. 5. The difference between the magnitudes of Q_{paddle}^{-1} and Q_{bare}^{-1} is large compared with the scatter in the low temperature Q_{bare}^{-1}, indicating that Q_{film}^{-1} obtained using Eq. (7) is reliable.

The Al Q_{film}^{-1} obtained from the data in Fig. 5 and Eq. (7) is plotted in Fig. 6, along with the prediction of the TM for single phonon relaxation rate prefactor $a=4.8\times10^8$ K^{-3} s^{-1} and tunneling strength $C=1.3\times10^{-4}$ (parameters defined in Sec. II B). Good agreement between these data and the TM was observed between 1 K and 10 mK. The Q^{-1} plateau observed in these data between 100 mK and 1 K is within the glassy range $2\times10^{-4} < Q^{-1} < 2\times10^{-3}$, indicating that the Al film conforms to the "universality" observed in nearly all amorphous solids.[9] As the temperature of our sample was lowered from 100 to 10 mK, the Q^{-1} of the Al film decreased. In the context of the TM, this "shoulder" at 100 mK

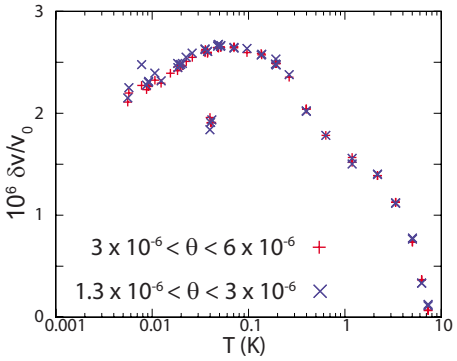

FIG. 8. (Color online) Measurements of $\delta v/v_0$ on the composite Al/Si resonator at two different strain levels, showing consistency between the results obtained at two different strains. The strains are within the range observed in the free decay of the Si/Ag resonator (Fig. 4) where the exponential behavior also is consistent with no strain dependence. The angle θ is defined in Fig. 3. The origin of the unreproducible points that deviate from the others around 30 mK is unclear.

is interpreted as a decrease in the relaxation rate of the dominant TLS below the driving frequency. Near 10 mK, the temperature dependence of Q_{film}^{-1} weakens, perhaps due to thermal decoupling. Thermalization and sources of heating in mechanical resonators at low temperatures are discussed in Refs. 40 and 41. The internal friction rises above the plateau level for temperatures well above 1 K, as in many amorphous solids.[42] This increase at relatively high temperatures has been attributed to thermally activated motion of TLS.[43]

The $\delta v/v_0$ of the Al film is shown in Fig. 7, along with the predictions of the TM for the same values of a and C that were used to fit to Q^{-1}. The data agree with the prediction of the TM for 10 mK$<T<$100 mK but the temperature dependence of $\delta v/v_0$ is stronger than that predicted by the TM between 100 mK and 1 K. The strong temperature dependence for $T>T_{CO}$ is also observed in amorphous SiO_2,[23] and it is not well understood theoretically. At temperatures above a few kelvins, a crossover to a linear temperature dependence is observed in amorphous solids[44] and disordered crystals.[42,45] $\delta v/v_0$ of our Al film decreases linearly between 5 and 12 K with a slope $\beta=-9\times10^{-5}$ K^{-1}, in agreement with the empirical relation[45] $\beta=0.5Q_0^{-1}$ K^{-1}, where Q_0^{-1} is the internal friction in the plateau region. The magnitude of $d(\delta v/v_0)/d(\log_{10} T)$ reaches a local minimum near $T_c=1.2$ K, perhaps due to the onset of electron-driven TLS relaxation (Table I) combined with the onset of an additional mechanism that leads to the linear temperature dependence of $\delta v/v_0$ at slightly higher temperatures.

Materials at very low temperatures often exhibit a nonlinear elastic response even at moderate strain amplitudes. It is therefore important to verify that data are taken in the linear regime. In the case of an amorphous solid, the nonlinearity results in a decrease in the elastic constants (softening) as strain is increased.[46,47] Figure 8 shows the relative change in sound speed of the composite Al-Si resonator at two different strain ranges. Since the range of strain values for our data in Fig. 7 coincides with the range of strains in Fig. 8, this figure shows that our results in Fig. 7 are not affected by strain dependence. A few points in Fig. 8 near 30 mK fall well outside the range of the rest of the data. They were all acquired in the time frame of a day and might be related to a particular operational condition. Checks on the data show that the shift in sound speed could not be reproduced.

Grain boundary and impurity contributions to Q^{-1} can be ruled out by the following arguments. Although grains in our polycrystalline Al film were visible at 100 times magnification, it was previously shown[8] that annealing a Cu film to decrease the total length of the grain boundaries resulted in an *increase* in Q^{-1} in the temperature range of the plateau. This indicates that grain boundaries do not significantly contribute to the dissipation. Although we did not carry out a similar annealing study for our aluminum films, we assume that the results for Cu carry over for Al films, and that most experiments that utilize similar metallic films for actuation and detection of mechanical resonators would forego the annealing step. It was also shown in Ref. 8 that impurity content was not responsible for the large Q_{film}^{-1} observed in metal films above 100 mK. Our Al film must be at least as pure as that studied in Ref. 8 since we deposited 5N purity Al in a dedicated chamber pumped to a base pressure below 10^{-7} Torr.

The tunneling strength C characterizing our Al film is about a factor of 2 less than in the often studied amorphous solid SiO_2.[23] This puts the tunneling strength for Al within the range of expected values for amorphous solids.[9] The relaxation rate prefactor a is larger in our Al film than in SiO_2 by a factor of 5. This could be due to differences in the TLS-phonon coupling γ or the sound speed v. In SiO_2 it has been shown that the ratio γ/v does not depend on phonon polarization,[24] and it is thus possible to determine γ_l and γ_t from a (γ is close to 1 eV for both polarizations). However, since only one mode of the bare paddle resonator has $Q^{-1}<10^{-6}$,[1] we could not study the dependence of γ/v on phonon polarization in the Al film. Also, the v^5 dependence makes a quite sensitive to the value of the sound speed. Since the dominant thermal phonon wavelength in Al exceeds the 1 μm thickness of the Al film below 40 mK,[48] the relevant sound speed is somewhere between that of Si and that of Al. It is thus not possible to determine whether the enhancement in a is due to differences between the values of γ or v in the Al film and SiO_2. An increase in γ relative to the value in SiO_2 would be expected because the width of the dislocation kinks in Al is large compared with the size of the defects in SiO_2, thus strengthening the coupling between the kinks and long-wavelength phonons.[29]

As mentioned in Sec. II, dislocation kinks may be responsible for the observed elastic properties. If the typical barrier height for kink motion were as low in Al as was calculated for Cu,[11] i.e., 2 mK, then thermally activated relaxation of TLS would be significant. However, thermally activated relaxation would produce a linear temperature dependence of Q^{-1} up to the temperature corresponding to the maximum barrier height, at which point a Q^{-1} maximum would exist.[49] Thermal activation is not expected to produce the plateau with a low-temperature drop off that we observe. In the context of the TM, the absence of thermal activation below 1 K would imply that the barrier for kink motion is typically greater than 1 K but the effective mass of the kink is low

enough so that tunneling can occur with a significant probability [Eq. (3)].

Other theoretical models do not seem to be consistent with our data. A radiation damping model was discussed in Refs. 50 and 51. In this model, the speed of the kinks' motion fluctuates as they are driven over the washboard and they radiate acoustic energy. In the theory in Ref. 50, the barrier height, stress energy, and kink-kink interaction energies are each taken to be much less than the temperature. Thus the relaxation times in the periodic potential must be fast compared to the drive frequency, making the out of phase, dissipative part of the response small. In the case where static strains introduce long-wavelength modulations in the kink potential that are comparable to or greater than the temperature, the kinks would adiabatically stay near local minima of the long-wavelength potential. The dissipation will then be dominated by transitions between these local minima, not by the damping due to transitions as the kinks are driven along the short-wavelength periodic potential.[29] The contribution to Q^{-1} due to vibrating edge dislocation dipoles was calculated within a modified Granato-Lücke string model in Ref. 52 but this resulted in a temperature independent Q^{-1} at low temperatures. Thus the theory, at least in its present form, is inconsistent with the sharp decrease in Q^{-1} that we observe between 10 and 100 mK.

B. Previous work: Aluminum

Pohl and co-workers[8,51,53] have studied the effect of plastic deformation on the acoustic and thermal properties of bulk Al. The plastic deformation is thought to produce a dislocation density $n_{disl}=(10^{11}\ \mathrm{cm}^{-2})\epsilon_{plas}$, where ϵ_{plas} is the plastic strain. The elastic properties were measured using the torsional oscillator technique with 2.5 mm diameter samples of 5N purity. The internal friction and magnitude of $d(\delta v/v_0)/d(\log_{10} T)$ increased up to dislocation densities of $\approx 10^{10}\ \mathrm{cm}^{-2}$ or $\epsilon_{plas}\approx 15\%$. Above this deformation level, it is thought that the dislocation density increased to a point at which dislocation-dislocation interactions limited further contributions to the acoustic properties. Measurements of Q^{-1} and $\delta v/v_0$ for 1% and 15% plastically deformed and annealed Al from Ref. 8 are shown in Figs. 6 and 7. The Q^{-1} of the 15% deformed Al is near the glassy range,[8] which spans $2\times 10^{-4}<Q^{-1}<2\times 10^{-3}$ and is close to the Q^{-1} of our Al film between 100 mK and 1 K. As in Ref. 8, we take this as evidence that the origin of the Q^{-1} in our Al film is related to dislocations. The $\delta v/v_0$ for the deformed Al decreases as the temperature increases from 100 mK to 1 K, as expected for an amorphous solid oscillating at kilohertz frequencies, but the data in fact have a linear temperature dependence. This is observed in amorphous solids as well, albeit at temperatures above a few kelvins.[44] Thus the elastic properties of highly deformed bulk Al are similar to those of an amorphous solid but there are significant departures from the predictions of the TM.

Measurements of the thermal properties of plastically deformed bulk Al reveal more substantial departures from the behavior of most amorphous solids.[53] The thermal phonon mean-free paths in pure e-beam deposited Al films and in 2.5 mm diameter, 5% deformed 5N bulk Al were determined from heat conduction measurements between 0.05 and 1.0 K. These measured mean-free paths are much smaller than those predicted by the TM based on the measured Q^{-1} in the temperature-independent region. In the case of the films, the discrepancy was greater than an order of magnitude. Even more surprisingly, while the internal friction in a molecular-beam epitaxial deposited silicon film with a nearly perfect structure was unmeasurably small, the thermal phonon mean-free path determined from heat conduction was within an order of magnitude of that of thermally evaporated a-SiO_2. For the a-SiO_2 film, the measured mean-free path and that predicted by the TM were in agreement. These results can only be compatible with the explanation of the elastic measurements on our Al film in terms of dislocation tunneling and the TM if some additional scattering process for thermal phonons exists in polycrystalline Al. However, it is not known what such a process could be.

Measurements of Q^{-1} and $\delta v/v_0$ for a single-crystal Al reed of unknown purity at 5.0 kHz are presented in Ref. 12 and reproduced in Figs. 6 and 7 (the work of Classen and co-workers). The approximate reed dimensions were 10 mm$\times$3 mm$\times$0.3 mm. The elastic properties do not agree with the TM,[12] though they are consistent with $\delta v/v_0$ and Q^{-1} for bulk Al with a deformation of at least 1% above 60 mK. The measurements on plastically deformed Al unfortunately do not extend below this temperature.

In Ref. 37, König *et al.* present measurements on a polycrystalline Al vibrating wire, and these also have some qualitative similarities to the predictions of the TM, although it is not possible to fit the TM to the data. These data, along with measurements on other polycrystalline metals, are also discussed in Ref. 54. The vibrating wire had a diameter of 25 microns, a length of a few millimeters, a resonant frequency of 7.7 kHz, and a purity of 4N. The wire was described as commercially available and no annealing was mentioned,[37] which indicates that it underwent considerable plastic strain during the manufacturing process, introducing a high density of dislocations. The $\delta v/v_0$ and Q^{-1} results are shown in Figs. 6 and 7. The Q^{-1} measured by König *et al.* agrees with the Q^{-1} of our Al film over almost the entire temperature range of overlap. König *et al.* also measure roughly equal slopes $d(\delta v/v_0)/d(\log_{10} T)$ on either side of the maximum in $\delta v/v_0$, as observed in other glasses, including amorphous SiO_2.[23,24] However, the maximum in $\delta v/v_0$ occurs at 250 mK, which is about five times the temperature of the maximum in $\delta v/v_0$ for our Al film. Thus the TM would predict a sharp decrease in Q^{-1} below 250 mK while the measurement shows only a weak decrease below this temperature. Since a substantial change in $\delta v/v_0$ was observed in a 5 μm diameter Al wire vibrating at 323 Hz as strain was increased from 7×10^{-7} to 2×10^{-6},[37] it seems likely that the measurements on the 25 micron diameter wire taken at a strain of $\approx 9\times 10^{-5}$ were also strain dependent.

Haust *et al.*[38] measured the acoustic properties of a pure polycrystalline Al reed vibrating at 2.6 kHz between 0.05 and 4 K. No details are given regarding the purity of the sample or the degree of deformation (e.g., during manufacturing). The geometry of the sample was chosen so that clamping loss did not limit the quality factor: an Al 5056

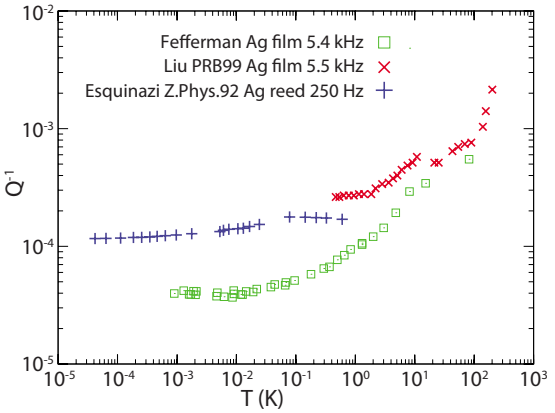

FIG. 9. (Color online) Q^{-1} measurements of our Ag film, the Ag film studied by Liu *et al.* (Ref. 8) and the Ag reed studied by Esquinazi *et al.* (Ref. 57).

vibrating reed with the same geometry was found to have over three times lower Q^{-1} at 100 mK than the pure Al reed in zero magnetic field. The zero-field results for pure Al are plotted in Figs. 6 and 7. The magnitude of Q^{-1} at the lowest temperatures is consistent with that expected for a plastic deformation of less than 1%. However, unlike the Q^{-1} of systematically deformed bulk Al, the Q^{-1} of the vibrating reed[38] is nearly temperature independent over the entire range of measurement. The temperature dependence of $\delta v/v_0$ in the same sample is consistent with a deformation of less than 1%. Since no significant decrease in Q^{-1} was observed at the lowest temperatures of the measurement, it is not possible to determine a best-fit value for a and check whether a fit to $\delta v/v_0$ is consistent with a fit to Q^{-1}.

In Ref. 8, Liu *et al.* studied Q^{-1} in several metal films, including Al, using the same double paddle resonator technique that we used. These data are shown in Figs. 6 and 7. The Al film they studied was also 1 μm thick, although electron-beam deposition with a substrate temperature below 100 °C was used. As shown in Fig. 6, at 200 mK the Q^{-1} of the Al film measured by Liu *et al.* is three times lower than the Q^{-1} of our Al film, perhaps due to the lower temperature of our film during deposition. Al films deposited at low temperatures are associated with greater microscopic disorder compared with films deposited at room temperature, as evidenced by higher resistivity, even if the films are annealed at room temperature.[55,56] Our measurements of $\delta v/v_0$, however, agree over the entire temperature range at which data are available, as shown in Fig. 7. Because the $\delta v/v_0$ measurements of Liu *et al.* only extend down to 500 mK, it is not possible to determine the degree to which the elastic properties of this film agree with the tunneling model predictions.

C. Ag film

The Q^{-1} of our Ag film between 1 mK and 100 K is plotted in Fig. 9. At 100 mK, Q^{-1} in our Ag film is three times below that in our Al film. As the temperature is decreased below 100 mK, the temperature dependence of Q^{-1} in our Ag film weakens, in contrast to the strong decrease in Q^{-1} of our Al film below 50 mK. The $\delta v/v_0$ for the Ag film is not plotted because our initial metal film data were not acquired with a view to exploring this quantity. The disagreement between our Ag results and the TM (Table I) does not invalidate the interpretation of our Al results in terms of the TM because the interaction between TLS and unpaired electrons may alter the temperature dependence of Q^{-1} in a nontrivial way (Sec. II B). Although some researchers argued that there is no difference between the low-temperature acoustic properties of polycrystalline Al in the normal and superconducting states,[37] implying that electrons do not affect the acoustic properties, subsequent work showed that there are substantial differences between $\delta v/v_0$ measured in the superconducting and normal states.[38] It was not possible to draw conclusions about the influence of unpaired electrons on Q^{-1} in Ref. 38 due to eddy current damping in the presence of the magnetic field.

As with the Al film, there are differences between the Q^{-1} of our Ag film and that of the Ag film measured in Ref. 8. At 1 K, the temperature dependence of Q^{-1} in our Ag film is stronger than that observed in Ref. 8, and the magnitude of Q^{-1} is three times smaller in our film. This difference is surprising because we tried to make the films as similar as possible, using the same e-beam evaporator, similar deposition rate, and probably the same e-beam target. The Q^{-1} of our Ag film is also different from that of a cold-rolled Ag reed vibrating at 250 Hz.[57] In the reed, Esquinazi and coworkers observed a Q^{-1} plateau between approximately 600 and 60 mK and $Q^{-1} \propto T^{1/3}$ between 0.1 and 60 mK, after subtracting a background contribution of 1.12×10^{-4}. The background contribution is over an order of magnitude greater than the internal friction at the lowest temperatures. It is claimed in Ref. 57 that Q^{-1} of the Ag reed is qualitatively the same as in the amorphous dielectric Suprasil but Q^{-1} of our sample has important differences: we do not observe a plateau between 100 mK and 1 K, and the strength of the temperature dependence of Q^{-1} uniformly decreases as temperature decreases below 10 K.

V. CONCLUSION

Using a low Q^{-1} single-crystal substrate vibrating in the linear regime, we measured damping in a high-purity polycrystalline Al film and found Q^{-1} orders of magnitude greater than that observed in annealed bulk Al. The mechanism leading to this high level of dissipation must be an internal process since our measurement technique was previously shown to be insensitive to interfacial and surface contributions. Grain boundary and impurity contributions to the damping were also found to be insignificant, leaving dislocation kinks as the defects most likely to be responsible for the high level of damping. It is not clear whether differences in dislocation density are responsible for the considerable variation in Q^{-1} across measurements on Al polycrystals by different researchers since the defect density was not well characterized except where the sample was intentionally deformed. This variation is substantial: the Q^{-1} we measured in our polycrystalline Al film is over an order of magnitude greater than that measured in a polycrystalline sample as reported in Ref. 38. Though the temperature dependence of Q^{-1} in our Ag

film is different from that in our Al film, the magnitudes of Q^{-1} are similar in the two films (within a factor of 3).

Though it is apparent from our results that a polycrystalline Al film hundreds of times thinner than its substrate can dominate the elastic properties of a composite resonator at audio frequencies, some recent work shows a decrease in damping for smaller dimensions or higher excitation frequency. $Q^{-1}<10^{-6}$ was observed in a nanomechanical SiN resonator coated with a polycrystalline Al film of comparable thickness.[5] Though a careful analysis has not been carried out, it is thought that the Q^{-1} of the Al coating is comparable to that of the composite structure. In measurements on Au nanomechanical resonators,[6] $Q^{-1}<10^{-5}$ was observed near 10 mK, though results for Au are not directly comparable to results for Al due to unpaired electrons in the former.

The elastic properties of our Al film are mainly consistent with the predictions of the TM for the case in which relaxation of tunneling states is dominated by phonons. The absence of electron-assisted relaxation is sensible since the temperature range in which the TM fits the data is below Al T_c and paired electrons do not contribute to TLS relaxation. The relative slowness of the phonon-driven relaxation accounts for the crossover at $T_{CO}\approx 50$ mK. If the TM predictions are compared with the previous Al measurements, it is clear that the annealed Al does not agree with the TM predictions while the 15% deformed Al is close to the TM prediction. It would thus be very interesting to extend the measurements on plastically deformed Al to lower temperatures and check for agreement with the TM. It is not possible to use Q^{-1} of our Ag film to rule out the TM because of the uncertain effect of unpaired electrons.

Though the model of tunneling dislocation kinks suggests an origin for tunneling TLS in polycrystals, it cannot rigorously explain both thermal and elastic measurements. The excess specific heat with linear temperature dependence and time-dependent heat release predicted by the TM is not observed in plastically deformed Al.[51] The lack of glassy anomalies in the specific heat and heat release might be explained in terms of the TM by an abundance of symmetric tunneling states relative to asymmetric tunneling states,[51] as would be expected if TLS form at the minima of long-wavelength modulations of the kink-Peierls potential. However, the phonon mean-free path in Al films derived from heat-conductivity measurements[53] is much shorter than that predicted by the TM based on the measurements of Q^{-1} in Ref. 8. Thus we are not aware of any completely satisfactory theory of the elastic properties of polycrystalline metal at low temperatures. From an empirical standpoint, we emphasize the important contribution of metal films to the damping of mechanical resonators at low temperatures.

ACKNOWLEDGMENTS

We wish to acknowledge very helpful discussions with Tom Metcalf and Xiao Liu of the U.S. Naval Research Laboratory and Bruce White of Binghamton. Jared Hertzberg assisted with the Al film deposition using an evaporator in the K. C. Schwab laboratory at Cornell. We acknowledge support from the NSF under Grants No. DMR-0457533 and No. DMR-0806629, and by DARPA under Grant No. HR0011-06-1-0042.

*jmp9@cornell.edu

[1] C. L. Spiel, R. O. Pohl, and A. T. Zehnder, Rev. Sci. Instrum. **72**, 1482 (2001).
[2] R. G. Knobel and A. N. Cleland, Nature (London) **424**, 291 (2003).
[3] X. L. Feng, C. A. Zorman, M. Mehregany, and M. L. Roukes, Solid-State Sensors, Actuators, and Microsystems Workshop, 2006 (unpublished), p. 86.
[4] M. D. LaHaye, J. Suh, P. M. Echternach, K. C. Schwab, and M. L. Roukes, Nature (London) **459**, 960 (2009).
[5] J. Hertzberg, T. Rocheleau, T. Ndukum, M. Sawa, A. Clerk, and K. Schwab, Nat. Phys. **6**, 213 (2010).
[6] A. Venkatesan, K. J. Lulla, M. J. Patton, A. D. Armour, C. J. Mellor, and J. R. Owers-Bradley, Phys. Rev. B **81**, 073410 (2010).
[7] I. W. Martin *et al.*, Class. Quantum Grav. **26**, 155012 (2009).
[8] X. Liu, E. J. Thompson, B. E. White, and R. O. Pohl, Phys. Rev. B **59**, 11767 (1999).
[9] R. O. Pohl, X. Liu, and E. J. Thompson, Rev. Mod. Phys. **74**, 991 (2002).
[10] D. R. Southworth, R. A. Barton, S. S. Verbridge, B. Ilic, A. D. Fefferman, H. G. Craighead, and J. M. Parpia, Phys. Rev. Lett. **102**, 225503 (2009).
[11] T. Vegge, J. P. Sethna, S.-A. Cheong, K. W. Jacobsen, C. R. Myers, and D. C. Ralph, Phys. Rev. Lett. **86**, 1546 (2001).
[12] J. Classen, M. Hübner, C. Enss, G. Weiss, and S. Hunklinger, Phys. Rev. B **56**, 8012 (1997).
[13] P. W. Anderson, B. I. Halperin, and C. M. Varma, Philos. Mag. **25**, 1 (1972).
[14] W. A. Phillips, J. Low Temp. Phys. **7**, 351 (1972).
[15] B. Golding, J. E. Graebner, A. B. Kane, and J. L. Black, Phys. Rev. Lett. **41**, 1487 (1978).
[16] J. L. Black and P. Fulde, Phys. Rev. Lett. **43**, 453 (1979).
[17] W. A. Phillips, Rep. Prog. Phys. **50**, 1657 (1987).
[18] J. Sethna, *Statistical Mechanics: Entropy, Order Parameters and Complexity* (Oxford University Press, Oxford, 2006).
[19] A. Fefferman, Ph.D. thesis, Cornell University, 2009.
[20] A. K. Raychaudhuri and S. Hunklinger, Z. Phys. B: Condens. Matter **57**, 113 (1984).
[21] P. Doussineau, C. Frénois, R. G. Leisure, A. Levelut, and J.-Y. Prieur, J. Phys. France **41**, 1193 (1980).
[22] This table corrects and supplements a similar table in Ref. 58.
[23] A. D. Fefferman, R. O. Pohl, A. T. Zehnder, and J. M. Parpia, Phys. Rev. Lett. **100**, 195501 (2008).
[24] J. Classen, T. Burkert, C. Enss, and S. Hunklinger, Phys. Rev. Lett. **84**, 2176 (2000).
[25] M. A. Ramos, R. König, E. Gaganidze, and P. Esquinazi, Phys. Rev. B **61**, 1059 (2000).

[26] R. König, M. A. Ramos, I. Usherov-Marshak, J. Arcas-Guijarro, A. Hernando-Mañeru, and P. Esquinazi, Phys. Rev. B **65**, 180201 (2002).
[27] W. Arnold, P. Doussineau, C. Frénois, and A. Levelut, J. Phys. Lett. (Paris) **42**, L289 (1981).
[28] K. A. Topp, E. J. Thompson, and R. O. Pohl, Phys. Rev. B **60**, 898 (1999).
[29] J. P. Sethna (private communication).
[30] T. H. Metcalf (private communication).
[31] K. R. Williams and K. Gupta, J. Microelectromech. Syst. **12**, 761 (2003).
[32] M. S. Kulkarni and H. F. Erk, J. Electrochem. Soc. **147**, 176 (2000).
[33] K. G. Lyon, G. L. Salinger, C. A. Swenson, and G. K. White, J. Appl. Phys. **48**, 865 (1977).
[34] F. Pobell, *Matter and Methods at Low Temperatures* (Spring-Verlag, Berlin, 1992).
[35] T. H. Metcalf, Ph.D. thesis, Cornell University, 1991.
[36] J. Wortman and R. Evans, J. Appl. Phys. **36**, 153 (1965).
[37] R. König, P. Esquinazi, and B. Neppert, Phys. Rev. B **51**, 11424 (1995).
[38] J. Haust, M. Burst, R. Haueisen, and G. Weiss, J. Low Temp. Phys. **137**, 523 (2004).
[39] B. E. White, Ph.D. thesis, Cornell University, 1996.
[40] E. Nazaretski, R. D. Merithew, R. O. Pohl, and J. M. Parpia, Phys. Rev. B **71**, 144201 (2005).
[41] A. Fefferman, R. O. Pohl, and J. M. Parpia, J. Low Temp. Phys. **148**, 875 (2007).
[42] K. A. Topp and D. G. Cahill, Z. Phys. B: Condens. Matter **101**, 235 (1996).
[43] K. S. Gilroy and W. A. Phillips, Philos. Mag. B **43**, 735 (1981).
[44] G. Bellessa, Phys. Rev. Lett. **40**, 1456 (1978).
[45] B. White, Jr. and R. O. Pohl, Z. Phys. B: Condens. Matter **100**, 401 (1996).
[46] D. Parshin, Z. Phys. B: Condens. Matter **91**, 367 (1993).
[47] J. T. Stockburger, M. Grifoni, and M. Sassetti, Phys. Rev. B **51**, 2835 (1995).
[48] T. Klitsner and R. O. Pohl, Phys. Rev. B **36**, 6551 (1987).
[49] S. Rau, C. Enss, S. Hunklinger, P. Neu, and A. Würger, Phys. Rev. B **52**, 7179 (1995).
[50] A. Hikata and C. Elbaum, Phys. Rev. B **9**, 4529 (1974).
[51] W. Wasserbäch, S. Abens, S. Sahling, R. O. Pohl, and E. Thompson, Phys. Status Solidi B **228**, 799 (2001).
[52] D. V. Churochkin, S. Sahling, and V. A. Osipov, Phys. Rev. B **72**, 014116 (2005).
[53] P. D. Vu, X. Liu, and R. O. Pohl, Phys. Rev. B **63**, 125421 (2001).
[54] P. Esquinazi and R. König, in *Tunneling Systems in Amorphous and Crystalline Solids*, edited by P. Esquinazi (Springer, Berlin, 1998), Chap. 4.
[55] A. D. C. Grassie and D. B. Green, J. Phys. C **3**, 1575 (1970).
[56] A. F. Mayadas, J. Appl. Phys. **39**, 4241 (1968).
[57] P. Esquinazi, R. König, and F. Pobell, Z. Phys. B: Condens. Matter **87**, 305 (1992).
[58] R. N. Kleiman, G. Agnolet, and D. J. Bishop, Phys. Rev. Lett. **59**, 2079 (1987).